JOURNAL OF MATERIALS SCIENCE 20 (1985) 3906–3916

Mechanical properties and phase diagrams of alloys of high density polyethylene with some low molecular weight organic compounds

B. HAGSTRÖM
Department of Polymeric Materials, Chalmers University of Technology, S-412 96 Gothenburg, Sweden

This paper reports on measurements of mechanical properties (stress–strain data) of four alloys based on high density polyethylene (PE) in combination with low molecular weight (LMW) organic compounds, together with the corresponding phase diagrams and microstructures. Two of the alloys, 1,2,4,5-tetrachlorobenzene (TCB)/PE and camphor/PE form eutectic structures. The system dimethylterephalate (DMTP)/PE also forms a eutectic but in this case the LMW component has only limited solubility in molten PE. In the thymol/PE system the LMW component acts as a low melting diluent. Apart from some primary grown crystals (camphor, TCB and DMTP), these systems were found to exhibit finely dispersed structures. The LMW additives (TCB and DMTP) with a modulus higher than pure PE impart a higher stiffness to the alloys while the strength and ductility remain approximately unaffected. The softer compounds (camphor and thymol) appear to act as softeners bringing about a decrease in tensile strength and an increase in ductility. The results obtained show that alloying of polymers with suitable LMW substances may represent a novel route to polymer-based composites. The occurrence of maxima in the elastic moduli of such alloys in the vicinity of the eutectic point illustrates the potential of such alloying as a means of modifying the properties of the matrix material.

1. Introduction

During recent years, there has been an increased interest in alloys based on polymers and low molecular weight organic compounds, in particular alloys of the eutectic type. Examples of such systems are 1,2,4,5-tetrachlorobenzene/PE [1–3], pentaerythrityl tetrabromide/polypropylene (PP) [4], 1,2,4,5-tetrachlorobenzene/PP [8], hexamethylbenzene/adamantane/PE [6], pentaerythrityl tetrabromide/poly(L-latic acid) [7], glutaric acid/poly(ethylene oxide) (PEO) [8], trioxane/poly(ε-caprolactone [9] and ethylene glycol based aliphatic polyesters containing a variety of low molecular weight diluents [10–15]. Further examples may be found in [16].

In the above work [1–15] interest has been focused mainly on the melting point depression and the resulting phase diagrams, crystallization kinetics, and the morphological factors. No investigation seems to have been carried out on the mechanical properties of alloys consisting of a polymer and a low molecular weight (LMW) organic compound.

The aim of this paper is to report on the mechanical properties (stress–strain data) of four alloys based on high density PE with a relatively high molecular weight, together with the corresponding phase diagrams and microstructures. Two of the alloys studied, 1,2,4,5-tetrachlorobenzene (TCB)/PE and camphor/PE

0022–2461/85 $03.00 + .12

form eutectic structures, while dimethylterephtalate (DMTP)/PE is an example of a system with a limited solubility in the liquid state. In the system thymol/PE, the LMW component acts as a low melting diluent (T_m = 50° C). The viscoelastic properties (stress relaxation) of the systems camphor/PE, DMTP/PE and thymol/PE have been reported elsewhere [17].

The LMW additives with a relatively high modulus value (TCB and DMTP) convey a high stiffness to the corresponding PE-based alloys. The "softer" LMW compounds (camphor and thymol) appear to act as softeners. The ultimate mechanical parameters also depend on the mutual solubility of the phases involved, a maximum in, primarily, the modulus being observed in some cases (camphor and TCB) in the vicinity of the eutectic point.

2. Experimental details

2.1. Materials

Two grades of PE were used, a high molecular weight material DMDS 2215 (Unifos Kemi AB), density 0.953 g cm^{-3}, melt flow index (MFI) 0.1 g 10 min^{-1}, $\bar{M}_w$ = 285 000, $\bar{M}_n$ = 22 000 (from GPC), and a material with a density of 0.962 g cm^{-3}, MFI 6.0 g 10 min^{-1}, $\bar{M}_w$ = 101 450, and $\bar{M}_n$ = 6180, Rigidex 50 (BP Chemicals International Ltd). The latter grade was used only in supplementary measurements concerning the phase diagrams.

The LMW compounds were analytical grades of camphor, 1,2,4,5-tetrachlorobenzene (TCB), thymol, and dimethylterephthalate (DMTP) with melting points of 178, 140.5, 50 and 141° C, respectively.

2.2. Sample preparation and mechanical testing

Two types of samples were used. For the systems camphor/PE, thymol/PE, DMTP/PE and TCB/PE, sheets (150 mm × 100 mm × 2 mm) were compression-moulded (0.5 MPa, 200° C, 50 min) in a mould designed to avoid sublimation. The cooling rate was about 10° C min^{-1}. Owing to blistering it was not possible to produce sheets of TCB/PE with a TCB concentration exceeding 30%; instead cylindrical billets (6.2 mm × 60 mm) were compression-moulded (50 MPa, 200° C, 30 min). The powdered components were carefully mixed prior to moulding.

The stress–strain measurements were performed on tensile test bars (ASTM D638, type IV) cut from sheets at room temperature (RT 22° C ±0.5) with a conventional tensile tester (Instron model 1193) equipped with an extensometer with a gauge length of 25 mm. The tensile Young's modulus was evaluated as the tangent to the stress–strain curve at zero strain. The strain rate was 4.2 × 10^{-4} sec^{-1}. Tensile stress and elongation at yield were determined at a strain rate of 2.1 × 10^{-2} sec^{-1}. The results given below are averages of seven parallel measurements.

The cylindrical samples for the system TCB/PE were tested dynamically in a "Dyna-Stat" device (Imass, Accord, Massachusetts, USA) at room temperature (RT). The real part of the complex modulus was recorded at 1 Hz at a maximum strain of 0.15%.

2.3. Thermal measurements and microstructures

The phase diagrams of the various systems were based on DTA measurements (Mettler TC 2000). The instrument was calibrated according to standard procedures. Homogeneous solutions of LMW/PE (*c.* 5 mg) were prepared by heating the mixtures in sealed aluminium pans at 200° C for 30 min. Subsequently, crystallization (T_c) and melting temperatures (T_m), taken as the peak values from the DTA thermograms, were recorded at different scan speeds. The T_m and T_c values were compensated for the influence of the heating and cooling rate.

The scanning electron micrographs (SEM) were obtained with fractured specimens cooled in liquid nitrogen using a Jeol JSM-35 microscope. Before the micrographs were taken the LMW component in the fracture surface was removed by sublimation at 50° C.

3. Results

3.1. Phase diagrams

3.1.1. Camphor/PE

Mixtures of PE with camphor were found to exhibit the features of a simple eutectic system. This is evident from Fig. 1, which also shows the influence of cooling rate prior to the heating scan in the DTA device. As expected, the melting points at the PE side of the diagram are suppressed by increasing the cooling rate. The eutectic temperature for 1 and 10° C min^{-1} cooling rate, and quenching are 121, 119 and

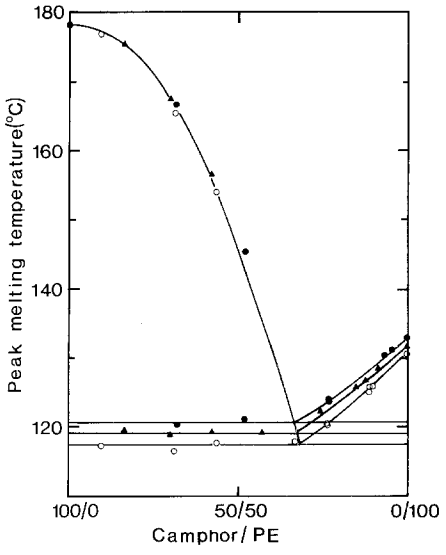

Figure 1 Peak melting temperature for the system camphor/PE. Samples cooled at 1°C (●), 10°C min^{-1} (▲), and quenched (○), heating rate 5°C min^{-1}.

117.5°C, respectively. On the other hand, the composition at eutectic point does not change measureably (67% PE). Owing to the uncertainty in drawing the eutectic horizontal and the liquidus curves, the error in estimating the eutectic composition was *c.* ±2%.

The absence of experimental points relating to the eutectic structure at PE concentrations exceeding 70% is explained by insufficient resolution of the eutectic and PE peaks in the DTA thermograms. Examples of such thermograms are shown in Fig. 2. For a mixture containing 76% PE, the melting of the eutectic phase is evident as a shoulder on the melting peak. At high PE concentrations, this shoulder disappears. Fig. 2 also shows examples of thermograms for other compositions, illustrating the measuring background of the method used.

The above results relate to a heating rate of

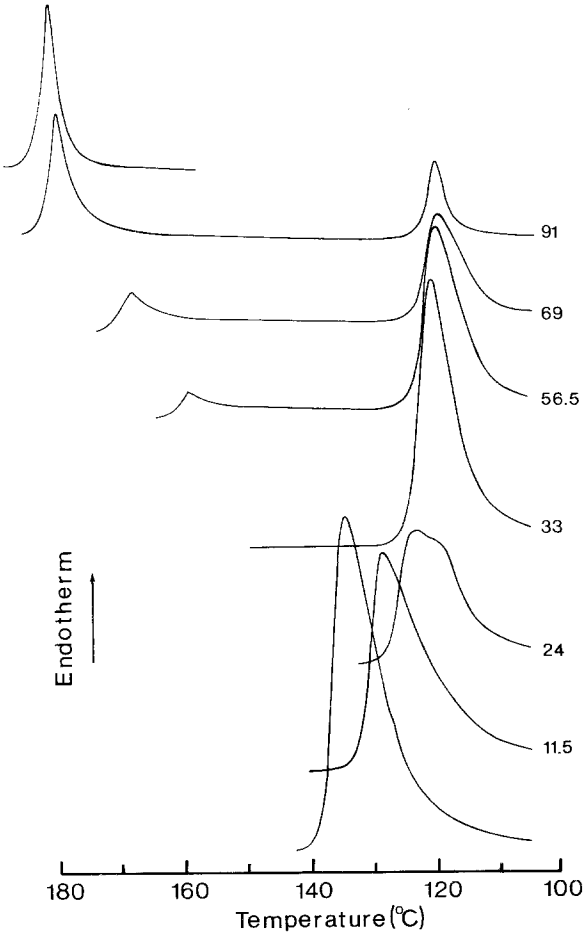

Figure 2 DTA-endotherms for quenched samples of camphor/PE. Heating rate 5°C min^{-1}. Figures indicate % camphor.

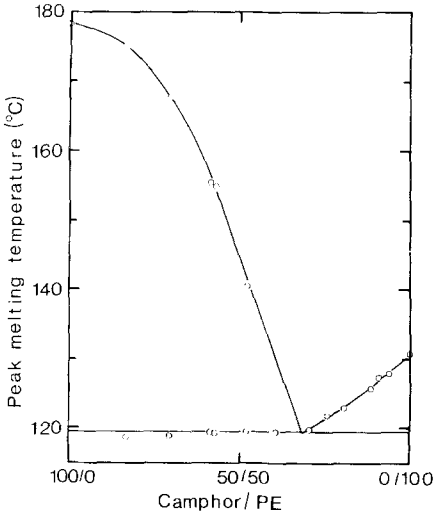

Figure 3 Peak melting temperatures for the system camphor/PE (M_w 101 000). Quenched samples, heating rate 5° C min^{-1}.

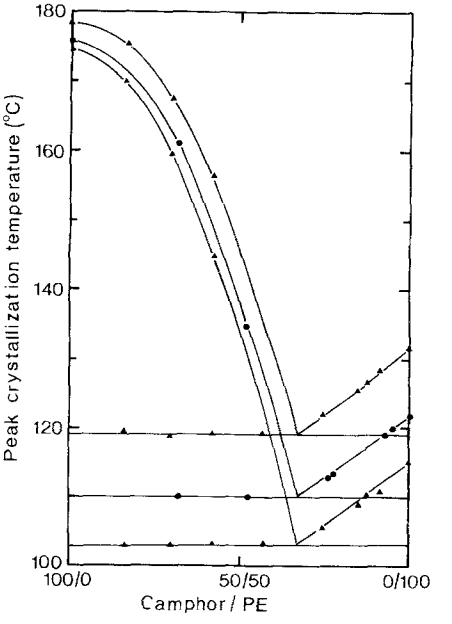

Figure 4 Peak crystallization temperatures for the system camphor/PE at 1° C (●), and 10° C min^{-1} (▲) cooling rate. Peak melting temperatures for mixtures cooled at 10° C min^{-1} are also included (upper curve).

5° C min^{-1}. When increasing this rate to 15° C min^{-1}, the eutectic temperature of a sample quenched from 200° C to RT was raised to 118.5° C (from 117.5° C, above). Again, the eutectic composition remained unaffected.

When using a PE grade with a lower molecular weight (*c.* 101 000) the camphor/PE diagram shown in Fig. 3 was obtained (quenched samples, 5° C min^{-1} heating rate). In this case, the eutectic horizontal was shifted slightly upwards (119.5° C), while the corresponding composition remained unaffected by the change in molecular weight of the PE component. Neither was there any change in the liquidus curve of camphor.

The data shown in Figs. 1 and 3 relate to the behaviour observed during heating (melting). The corresponding eutectic diagram for the camphor/PE system based on T_c is reproduced in Fig. 4. The various mixtures were homogenized thermally at 200° C in the DTA device, whereafter their exothermal peaks upon cooling at 1 and 10° C min^{-1} were recorded. For the sake of comparison, Fig. 4 also gives T_m values of the mixtures cooled from 200° C at 10° C min^{-1}. Fig. 4 shows a pronounced variation of the eutectic temperature with the rate of cooling (110 and 103° C, at 1 and 10° C min^{-1}). As was found for the melting scans, the eutectic composition remained unaffected by the cooling rate (67% PE).

Comparing the T_c and T_m values in Fig. 4 it is found that a constant supercooling of 10° C is required for crystallization for both the eutectic structure and the pure PE phase. For pure camphor the supercooling increases monotonically up to the eutectic composition (from 3 to 10° C).

3.1.2. TCB/PE

The phase diagram for the TCB/PE system has been established by Smith and Pennings [3]; it was found to be of a simple eutectic type with a eutectic composition of 55% PE (based on T_c). The PE material used in the present study behaved similarly. From a comparison between the systems TCB/PE and camphor/PE it is concluded that the overall characteristics of the phase diagrams are approximately the same.

3.1.3. DMTP/PE

In camphor/PE, the LMW component was completely soluble in the molten polymer. This is not true for the system DMTP/PE, as DMTP is only partly soluble in molten PE.

The T_m–composition diagram of the DMTP/PE system, shown in Fig. 5, is based on melting endotherms obtained on samples thermally homogenized at 200° C for 30 min, and quenched to RT. The heating rate was 5° C min^{-1}. T_c values at a cooling rate of

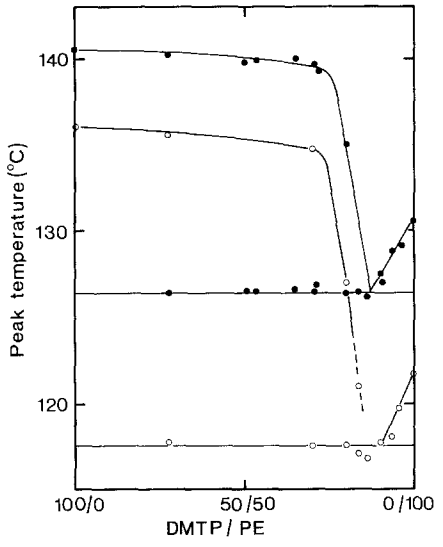

Figure 5 Peak melting and crystallization temperatures for the system DMTP/PE. Quenched samples, heating rate 5° C min^{-1}. Cooling rate 2° C min^{-1}.

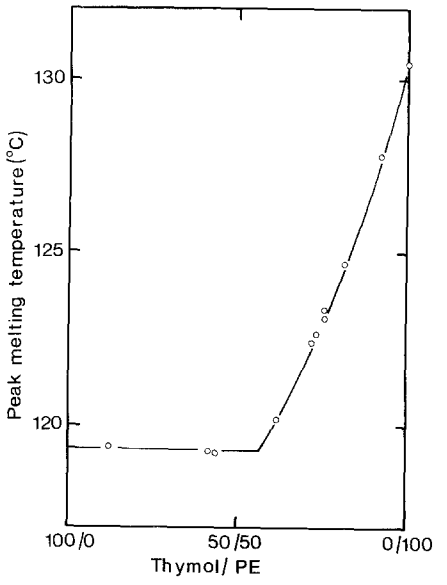

Figure 6 Peak melting temperatures for the system thymol/PE. Quenched samples, heating rate 5° C min^{-1}.

2° C min^{-1} are also included in Fig. 5. The limited solubility is reflected in a constant T_c for DMTP in the range of 0 to 70% PE. At higher concentrations the T_m and T_c values appear to decrease. In the range from *c.* 80 to 100% PE the DTA method used had a limited resolving power, a single melting endotherm only being recorded. However, the results indicate the existence of a simultaneous crystallization of DMTP and PE forming a eutectic structure. The eutectic composition appears to be located at 85 to 90% PE.

The limited solubility of DMTP in molten PE was also confirmed by direct microscopic studies (polarization, hot stage). At higher concentrations, complete solubility was achieved only at temperatures substantially above T_m of DMTP. When the temperature was lowered, small droplets of DMTP began to separate. The liquid–liquid separation as function of temperature and composition was not studied.

3.1.4. Thymol/PE

the T_m–concentration diagram for thymol/PE is given in Fig. 6. The data were obtained on samples quenched from 200° C to RT. The T_m value of pure thymol, 50° C, was not significantly affected by the presence of solid PE. The depression of T_m of PE amounts at most to 11° C at a concentration of about 45% thymol. Fig. 6 indicates that thymol is soluble in PE up to 45%; the solubility at higher concentrations was not studied. The DTA thermograms for pure PE and PE in the presence of thymol were slightly different in that the melting endotherm for PE showed a weakly developed shoulder located about 2.5° C below the main peak. This effect was not studied further.

Thymol is an easily supercooled compound; the samples crystallized completely only after storage at −20° C.

3.2. Microstructure

This section reports on some microscopic observations of the crystalline habits of the phases constituting the systems camphor/PE, DMTP/PE and thymol/PE.

3.2.1. TCB/PE

For the sake of completeness, we refer here to the work of Smith and Pennings [1–3] who studied the microstructure of different compositions in the eutectic system TCB/PE. The overall characteristics of the microstructures of the system TCB/PE are approximately the same as for the system camphor/PE except that TCB exhibits faceted growth.

3.2.2. Camphor/PE

Contrary to TCB, camphor grows into dendritic shapes both in its pure state and in solutions with PE. Fig. 7 shows a fracture surface of an

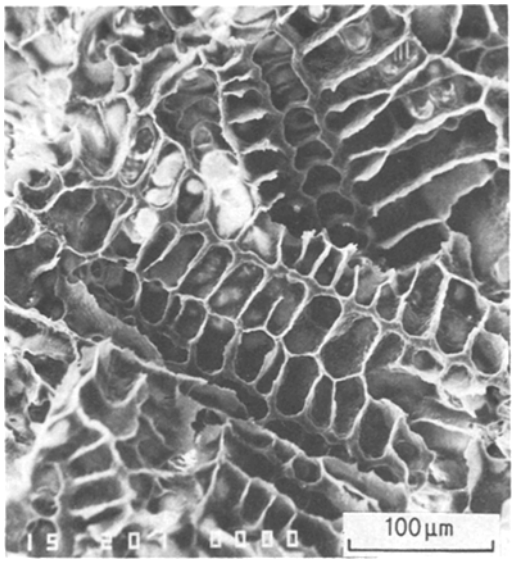

Figure 7 Scanning electron micrograph of the remaining, cellular PE matrix after removal of the camphor phase by sublimation. 85% camphor.

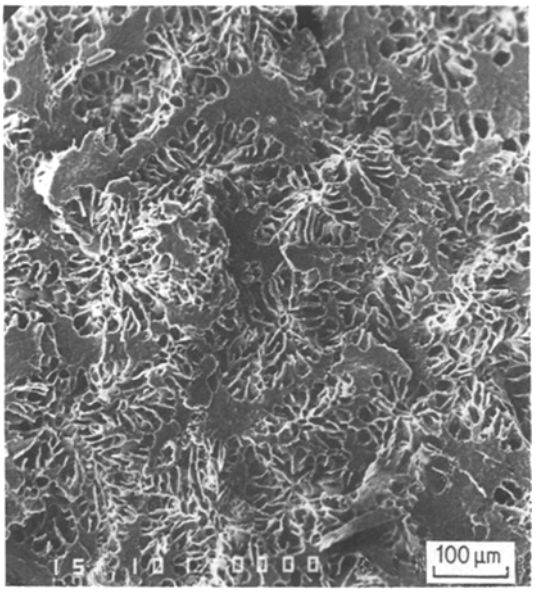

Figure 8 Scanning electron micrograph of the cellular PE matrix at 50% camphor.

85% solution of camphor in PE. The primary camphor crystals have grown relatively independent of the PE phase, giving rise to a highly cellular PE structure. At lower camphor contents the growth behaviour of the primary camphor crystals is altered into a spherulitic habit. This is shown in Fig. 8 where a micrograph of a 50% solution of camphor in PE is reproduced.

Fig. 9 shows a fracture surface obtained by breaking a tensile test bar of the camphor/PE eutectic. It is evident that the eutectic structure is finely dispersed. In the right hand part of Fig. 9 a more detailed micrograph is shown. The PE phase is arranged as a coarser superlattice connected with very thin intercrystalline fibrils.

3.2.3. DMTP/PE

Fig. 10 shows a fracture surface of an alloy with 20% DMTP. The primary faceted DMTP crystals are responsible for the fan-shaped structures. Intermediate regions form a finely dispersed structure. The right hand part of Fig. 10 is a fracture surface of an alloy with 10% DMTP. No signs of precipitated and primary grown DMTP are seen in this highly dispersed material.

3.2.4. Thymol/PE

In Fig. 11 a fracture surface of an alloy of 30% thymol in PE is shown together with a more detailed picture. The PE phase has a tube-like somewhat branched appearance, with spherical outgrowths. Again, the structure is finely dispersed.

3.3. Mechanical properties

In this section, we report on the measurements of some key mechanical parameters as evaluated from the stress (σ)–strain (ε) curves of the various mixtures. These parameters are the modulus of elasticity (E) and the stress and deformation at yield (σ_y, ε_y).

3.3.1. Camphor/PE

The variation of the modulus with the composition for the camphor/PE systems is reproduced in Fig. 12. On increasing the camphor concentration to around 10%, the modulus falls to about 60% of its initial value. In the 30 to 40% range, there is a maximum in E, approximately coinciding with the eutectic point (cf. Fig. 1). Fig. 12 also shows the theoretical variation of E when calculated from the simple upper (Voigt) and lower (Reus) bound theories. The corresponding relations are

$$E = v_1 E_1 + v_2 E_2 \qquad \text{(Voigt)} \qquad (1)$$

and

$$\frac{1}{E} = \frac{v_1}{E_1} + \frac{v_2}{E_2} \qquad \text{(Reuss)} \qquad (2)$$

Here E denotes the modulus of the composite, E_1

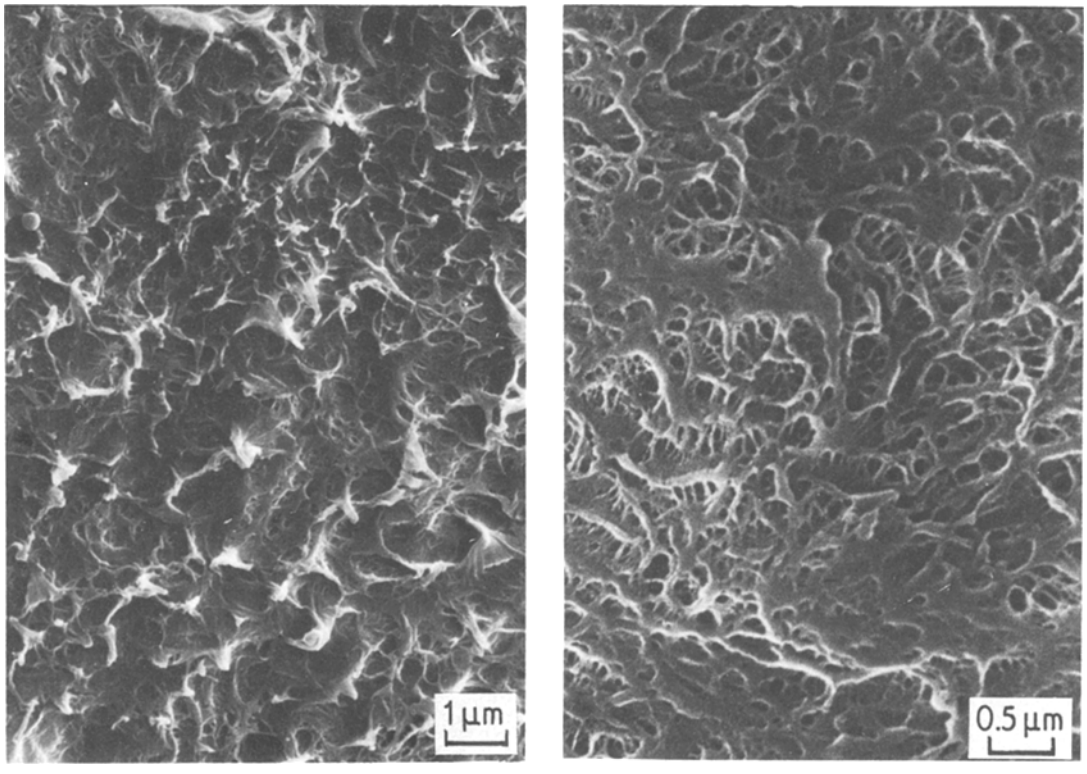

Figure 9 Scanning electron mocrographs of the eutectic structure at 32% camphor.

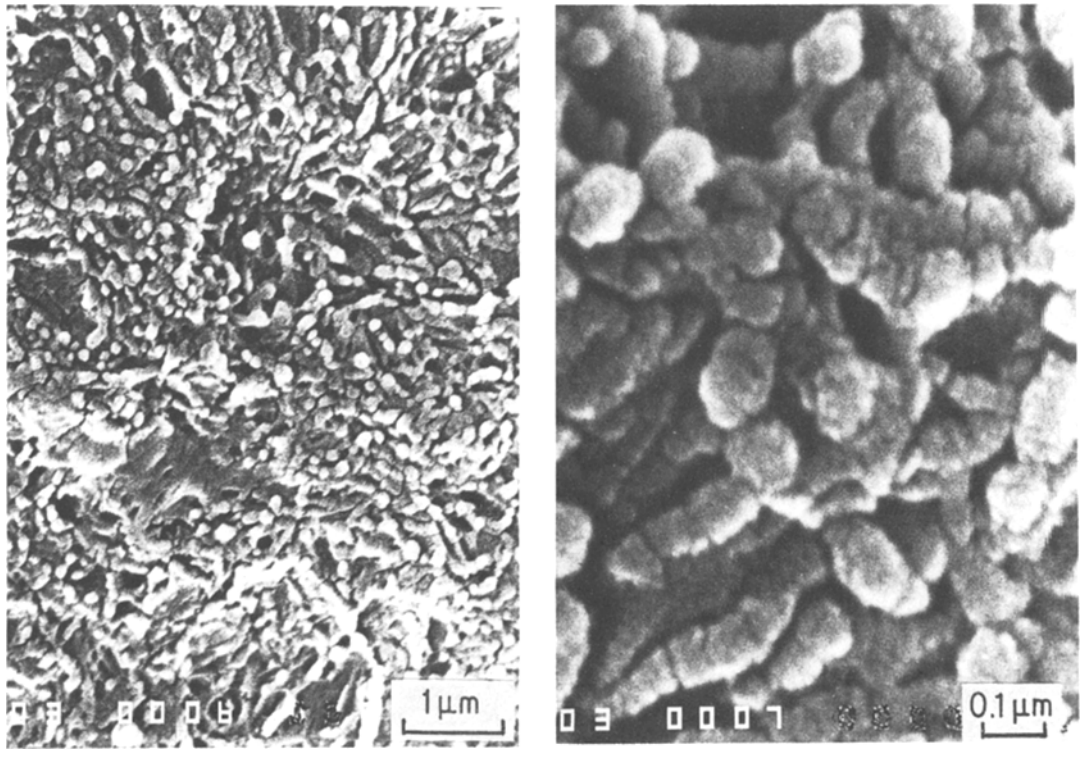

Figure 10 Scanning electron micrographs of the remaining PE phase at 30% thymol.

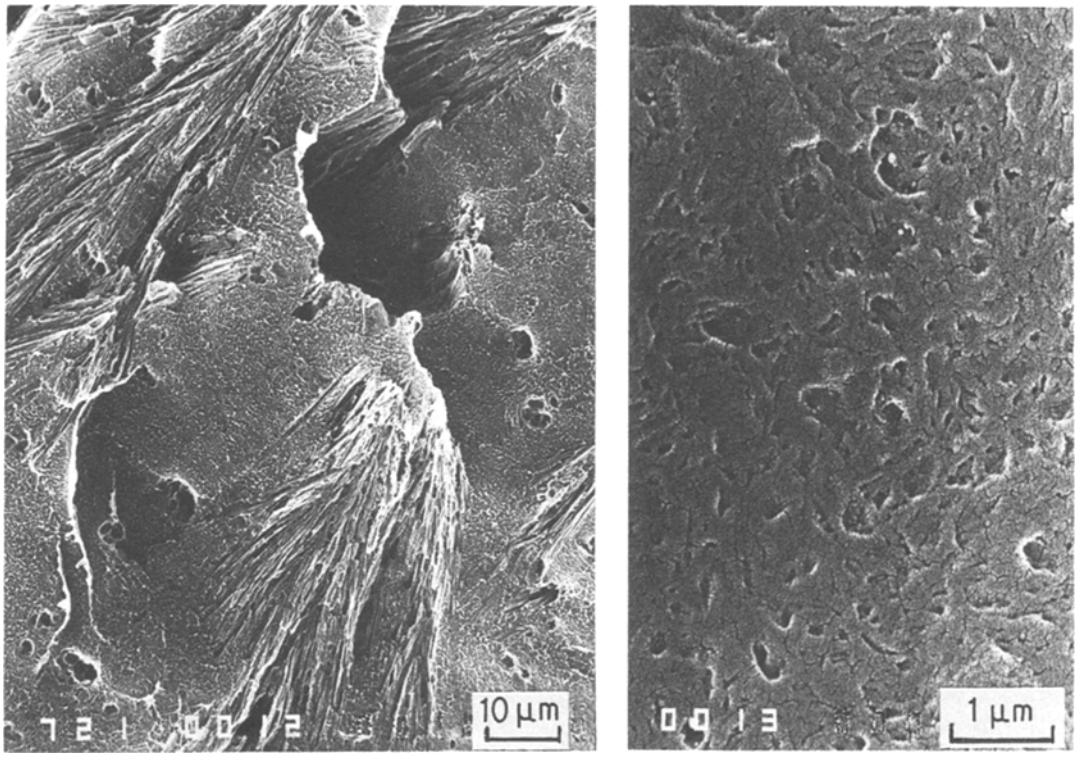

Figure 11 Scanning micrographs of the remaining PE phase at 20% (left) and 10% DMTP (right).

and E_2 the moduli of the components and v_1 and v_2 the corresponding volume fractions. The theoretical bounds shown in Fig. 12 has been obtained from Equations 1 and 2, neglecting the 4% difference in density between PE and camphor. The modulus value of pure camphor could not be determined from tensile experiments on compression moulded sheets. Instead, E was measured dynamically at 1 Hz on compression moulded (500 MPa, RT) cylindrical billets. The modulus ratio of camphor/PE measured in this way was 0.56, from which a modulus of 640 MPa is predicted and used in Fig. 12. The experimental data for the modulus falls outside the area between the theoretical upper and lower bounds (cf. Fig. 12). This indicates that the properties or the structure of the components may have been changed compared with those of the pure substances.

The σ–ε curves (at $\dot{\varepsilon} = 2.1 \times 10^{-2}\,\mathrm{sec}^{-1}$) for the various compositions in the camphor/PE system are shown in Fig. 13, the yield points being marked by arrows and fracture by crosses. There is a general decrease in the stress level with increasing camphor concentration. Fig. 14 summarizes the σ_y and ε_y values evaluated from the σ–ε curves of Fig. 13. There is a monotonic fall in σ_y with increasing camphor concentration. The ε_y values show an initial increase up to about 10% camphor, whereafter they start to decrease. There are no discontinuities in the vicinity of the eutectic concentrations. Necking was observed in alloys of up to 30% camphor.

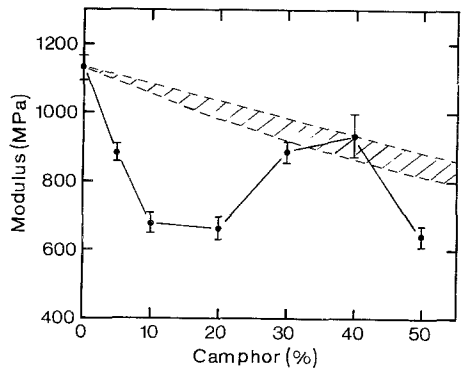

Figure 12 Modulus as a function of concentration for the system camphor/PE. The upper and lower bounds according to Equations 1 and 2 are included in the graph.

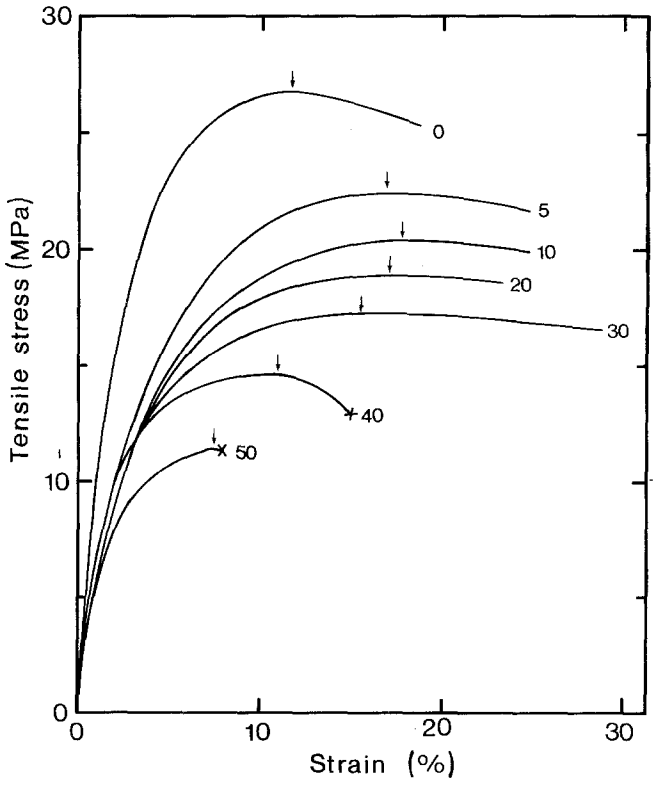

Figure 13 Stress–strain curves at $\dot{\varepsilon} = 2.1 \times 10^{-2}\,\mathrm{sec}^{-1}$ for the system camphor/PE. Camphor concentrations in per cent are indicated in the figure.

3.3.2. TCB/PE

Fig. 15 contains the results relating to the E, σ_y, and ε_y values as measured on the system TCB/PE. After a weakly developed minimum at low TCB concentrations (10%), the modulus increases up to 60% TCB whereafter it levels off. There is no discontinuity at the eutectic composition at 45% TCB. Both yield parameters behave similarly when the TCB concentration is increased, showing a sharp decline at concentrations above about 30%. This latter effect is due to difficulties in sample preparation (blistering). Necking was observed up to 30% TCB.

Measurement of the modulus of pure TCB was not possible due to the brittleness of the sample (breaking under the clamping force in the dynamical tester). This also applied to

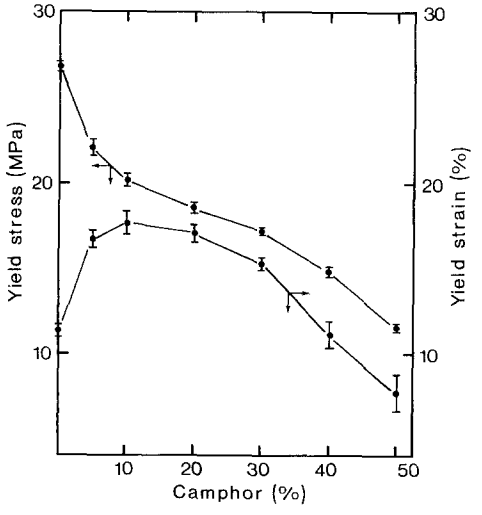

Figure 14 Tensile strength and per cent elongation at yield against concentration for the system camphor/PE.

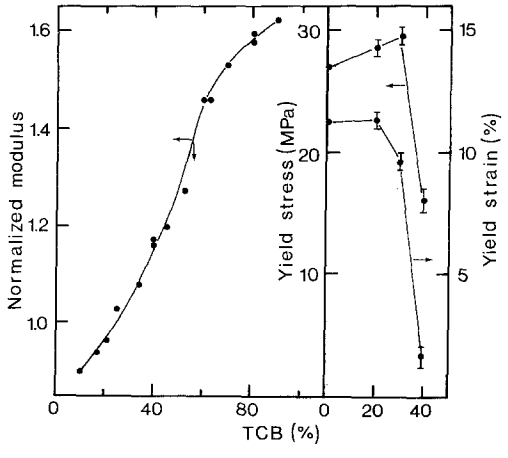

Figure 15 The real part of the complex modulus at 1 Hz, normalized with respect to pure PE, tensile strength, and per cent elongation at yield against TCB concentration.

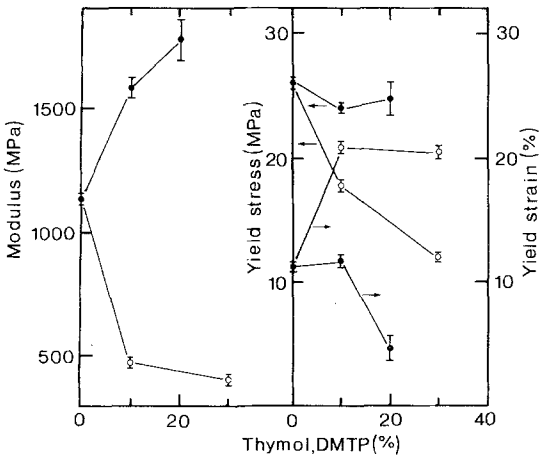

Figure 16 Modulus, tensile strength and per cent elongation at yield as a function of concentration for the system DMTP/PE (●) and thymol/PE (○). For 20% DMTP the samples fractured before yield.

DMTP and thymol. However, for TCB it seems possible to obtain the modulus for pure TCB by extrapolation in Fig. 15. The results for TCB/PE are reproduced here to supplement the phase diagram (eutectic) as reported in [3].

3.3.3. DMTP/PE, thymol/PE

The moduli for the systems DMTP/PE and thymol/PE are plotted in Fig. 16. While a substantial increase in E (*c.* 55% at 20% concentration) is recorded for DMTP, thymol has an even more pronounced weakening effect. The yield parameters of the DMTP system remain practically unchanged when 10% DMTP is added to PE. At 20% DMTP ε_y falls steeply, coinciding with the presence of primary DMTP crystals. The other system shows a decrease in σ_y, accompanied by an intitial (up to 10%) increase in ductility. It was not possible to increase the concentration above 20% DMTP, because of a non-uniform thickness of the compression-moulded samples. Necking was observed for all compositions, except for 20% DMTP.

As already mentioned it was not possible to measure the parameters in Fig. 16 on the corresponding pure LMW substances. However, preliminary measurements of the compression modulus, although not very accurate, clearly reveal that the pronounced variations in E could not alone be explained by the modulus value for the corresponding pure LMW substance.

4. Discussion

The phase equilibria in the system camphor/PE correspond largely to those found earlier with TCB/PE and a number of other PE-based systems [1, 5, 6, 8]. The camphor liquidus is largely indendent of kinetic factors (heating rate), while the PE branch behaves as pure PE with different thermal history. The rate insensitivity of the eutectic composition has been reported for a number of similar systems, especially with T_c based phase diagrams. Moreover, the values of 0.7 ± 0.07 for the polymer volume fraction at the eutectic points as found with TCB/PE, TCB/PP, and pentaerythrityl tetrabromide/PE (or PP) [4], was confirmed also for camphor/PE (0.68).

Unlike the composition, the temperature of the eutectic point is affected by the cooling rate, following the behaviour of pure PE. Further comments on the rate dependence of the PE-liquidus curve and the stability of the eutectic composition (TCB/PE) may be found in [1].

As pointed out by Smith and Pennings [3, 4], the crystalline habits of the various phases found in systems of this type may be associated with differences in diffusivity between the LMW and polymer components. Together with supercooling, these differences may result in segregated structures as, indeed, found here. In a camphor/PE alloy containing 40% of the LMW compound only a few small primary camphor crystals were found. The surrounding eutectic structure was segregated into coarser and finer regions. The tiny PE fibrils observed at the eutectic composition were absent both below and above this point. The structure formed from a melt with eutectic composition thus appears to be unique.

In the system thymol/PE the melting point of the LMW component is too low to allow eutectic crystallization. Despite this, the structure is highly dispersed.

A direct association of the mechanical properties with conventional concepts of composite structure is, in principle, possible only in cases where the components are insoluble in each other. Moreover in the systems studied here the moduli of the LMW componenets, could not be determined. An exception was the dynamical determination of E for camphor at 1 Hz. For TCB, an approximate E-value limit can be obtained from Fig. 15 at high TCB concentrations. From this, E for camphor amounts to

about half the value for the linear PE grade used, while TCB appears to be about twice as rigid as this PE grade. The E-value of the alloys follows, on the whole, a similar pattern, the camphor alloys being softer, the TCB-alloys harder than the polymer. For camphor and TCB, the dependence of E on the composition is not monotonic, there being a pronounced maximum at the eutectic points. One should also note the marked increase in E for the DMTP compositions. Like camphor, thymol produced a reduction in the modulus.

Owing to the closeness of the E-values of the components, the Voig/Reuss bounds for the modulus of the alloys enclose a relatively narrow area; the experimental E-values of the alloys fall far outside these bounds.

The pattern followed by the variation of the stress and strain at yield, σ_y and ε_y, is not easily interpreted. The more rigid LMW substances leave ε_y practically unchanged, while for the softer thymol and camphor one observed a higher ductility. The trends found with σ_y do not seem to allow any meaningful interpretation. On the whole, σ_y falls less than is usually the case with inert fillers at the corresponding concentrations.

Crystallinity changes of PE cannot account for the observed variation of the mechanical parameters since the crystalline fraction remained constant at around 65% (DTA analysis). This contradicts the findings of Smith and Pennings [1] who found a decrease from 64% to 48% for the eutectic point of the TCB/PE system.

Another factor which may influence the results is the formation of voids. This effect was not studied further.

Indications of solid solutions confined to the amorphous regions of the polymer phase have been obtained by Carbonnel *et al.* [10–15]. The present results do not permit conclusions about the possible occurrence of such solutions.

The LMW substances chosen for the present investigation constitute but a small extension of the range of substances reported earlier. TCB was selected in view of the previous work done on this substance [1–3], especially with regard to the TCB/PE phase diagram; the other substances were known (from qualitative tests) to exhibit different degrees of solubility with PE. Despite the limited number of the systems investigated, the results appear to show that the addition of low molecular weight organic substances to polymers may represent a novel route to polymer-based composites. The fact that the moduli of some of the alloys fall outside the usual Voigt/Reuss bounds supports the expectation of property changes beyond those obtainable with common fillers (*c.* Fig. 12).

Acknowledgements

Financial support from The Swedish Board for Technical Development is gratefully acknowledged. Thanks are also due to Professor J. Kubát for valuable advice in preparing the manuscript.

References

1. P. SMITH and A. J. PENNINGS, *Polymer* **15** (1974) 413.
2. A. J. PENNINGS and P. SMITH, *Brit. Polym. J.* **7** (1975) 460.
3. P. SMITH and A. J. PENNINGS, *J. Mater. Sci.* **11** (1976) 1450.
4. *Idem, J. Polym. Sci.* **15** (1977) 523.
5. P. SMITH, G. O. R. ALBERTA VAN EKENSTEIN and J. J. PENNINGS, *Brit. Polym. J.* **9** (1977) 258.
6. P. SMITH, R. KNOINGSVELD, C. J. H. SCHOUTETEN and A. J. PENNINGS, *ibid.* **12** (1980) 215.
7. R. VASANTHAKUMARI, *Polymer* **22** (1981) 862.
8. C. C. GRYTE, H. BERGMANS and G. SMETS, *J. Polym. Sci. Polym. Phys. Ed.* **17** (1979) 1295.
9. J. C. WITTMANN and R. ST. J. MANLY, *ibid.* **15** (1977) 1089.
10. C. PONGE, J. C. ROSSO, L. CARBONNEL and R. GUIEU, *Bull. Soc. Chim. France*, **8/9** (1970) 2849.
12. *Idem, ibid.* **8/9** (1970) 2855.
13. *Idem, ibid.* **3** (1972) 934.
14. *Idem, ibid.* **9/10** (1973) 2776.
15. *Idem, ibid.* **9/10** (1973) 2780.
16. B. WUNDERLICH, "Macromolecular Physics" (Academic Press, New York, 1980) Chs. 8 and 9.
17. B. HAGSTRÖM and J. KUBÁT, *J. Mater. Sci.* **19** (1984) 2606.

Received 5 April
and accepted 20 November 1984